

Design verification of optimized regenerative pylon with smart foot adapter for socio-economic backward classes with lower limb amputation

Palaiam Siddikali¹, Dr. P S Rama Sreekanth^{2*}

^{1,2} School of Mechanical Engineering, VIT AP University, Amaravati, A.P, 522237, India

Abstract

Lower limbs are exposed to an immense amount of impact forces during walking cadence and ambulators rely on various systems to shield the musculoskeletal arrangement from external shocks that inflict injury. The work elaborates the need for the adaptive design of Regenerative effort assistive Smart Pylon (RSP) with a Smart foot adapter (SFA) and wave spring suspension mechanism to resist static and dynamic impact load of 60-100 kgs amputee and also stabilizes to ground reaction forces (GRF) without falling. Stress maximum, axial, bending, and torsional stresses were assessed for Al 6061 T6 material and the related fatigue failure criteria were evaluated. The operating stress, deflection response, and wave spring rate of the pylon unit have been calculated and the pertaining results show that the designed RSP pylon unit is safe to impact forces and more favorable for impoverished lower limb amputees and to carry out their daily activities without compromising.

Keywords: Pylon, foot adapter, cadence, prosthesis.

1. Introduction

Lower limb prostheses are usually comprised of four major parts: Socket, knee, pylon, and foot as shown in Fig 1. The socket is a cup-shaped molded covering to the residual stump to safeguard the musculoskeletal arrangement by distributing the stresses produced by the mass of the amputee to the sidewalls of the socket then knee joint which encompasses a major task in maintaining overall body balance and provides the stability for anterior and posterior movement of the leg in case of A/K (above knee) amputees, but it is absent in case of B/K (below the knee) (**Jacobs, 1998**) amputees. The prosthetic shank/pylon is a portion connecting the foot- ankle joint assembly to the upper prosthesis, typically to the socket in B/K or the knee unit in A/K prosthetic legs. The main purpose of the pylon is to transfer the vertical loads caused by the mass (kg) of the amputee to the foot and then onto the ground.

The pylon profile, weight, and interfacing strategies are a couple of important concerns to manage, the shape of the pylon would involve features that would not probably hurt others or hurt the amputee person (**Buckley, Jones, & Birch, 2002**). Almost all prosthetic parts use a regular adapting methodology and unique designs with lighter weight to operate as intended, but uniqueness in pylon standards ought to be reflected. In general, the pylon and its adapter/connectors are made from aluminum and titanium alloys (**Kadhim Oleiwi & Jumaah Ahmed, 2016**) to reduce weight, increase strength, and withstand high impact forces. Specifically, the fatigue safety factor (FSF) of artificially aged, powder metallurgy 6061 aluminum alloy (**Lin, Hwang, & Fung, 2016**) was

discussed for the proposed pylon. To explore the pylon flexibility to ground reaction forces (GRF), shock absorber units are to be provided through passive mechanisms for repetitive, high-frequency impact events that occur throughout gait. A 3-dimensional gait analysis (**de Jong, Kerkum, van Oorschot, & Keijsers, 2020**) or a 2-dimensional video analysis with a force vector overlay can be used to measure the GRF in comparison to the joint rotation center of the knee and the endpoint distal link forces were estimated through force plates during ground contact at the stance event phase and were considered to be negligible during swing phases. However, these approaches are confined to lab conditions (**Koehler-mcnicholas, Lipschutz, & Gard, 2016**), costly and time-consuming, and error-prone, and thus not necessarily possible in outpatient clinics. As a replacement for the GRF concerning the joint center of the knee, a pylon tendency to a vertical angle with center of mass (COM) (**Soni, Maji, & Anand, 2010**), ankle moment, and dorsiflexion angle is proposed as a criterion for pylon-ankle tuning.



Figure. 1 A typical transfemoral prosthesis

The regular tubular pylon available in the market can't withstand high impact forces and does not provide comfort to the amputee and the patient needs to put more energy during the walk. To address the issue, a design verification research of the "RSP pylon with SFA" that was exposed in this paper combines axial, bending, and torsional loads and focuses on a probabilistic approach that uses fatigue failure rules. The bodyweight's of humans varying between 60- 100 kg, during slow, normal, and fast cadence are considered for design verification. For the wave spring design, the corresponding operating stresses, spring deflection, and other design parameters were assessed under different loads. Al 6061 T6 which is used to make the RSP pylon should withstand complicated states of stress concentration when exposed to bending, twisting, and axial loading during different walking cadence and loads and it results in stress gradients on the pylon surface, so to resolve this the wave spring (**Tekwani & Joshi, 2018**) with a lesser number of waves and a higher number of turns is incorporated in the RSP pylon unit.

2. Materials and Methods

2.1. Study design

The ergonomic A/K prosthesis model for the present study consists of the socket unit, knee unit, RSP unit, and foot with additional adapters to fit. This work only focuses on the Regenerative effort

Design verification of optimized regenerative pylon with smart foot adapter for socio-economic backward classes with lower limb amputation

assistive pylon with a smart foot adapter which will completely change the pylon environment and which safeguards the knee and socket unit by minimizing the amputee mass stress factors and the GRF. To provide additional retraction energy to walk with ease on the flat ground and the bumpy areas, wave spring arrangement will help and the total mechanism was described in the flowchart Fig 2. This advanced pylon will make a change in the amputee's comfort and performance to carry out their daily life activities.

Generally, the stance phase happens at 0 percent of the heel contact during the gait cycle and finally stops at approximately 60 percent of the toe-off gait. The swing event phase with the same leg lasts until the next foot touch, this will complete 100 percent of the gait cycle (**Pejhan, Farahmand, & Parnianpour, 2008**). During the stance phase, GRF's will act vertical and horizontal which may cause a moment at the ankle and which is directly transferred to the pylon part and then near the knee joint. At the heel contact event phase (HC) three stresses are generated in the pylon, they are bending (**Ávilaambriz, Almaraz, Gómez, & Juárez, 2015**), torsion (**Marno & Ismail, 2012**), and axial compression stress. At the mid-stance event (MST) phase the compression stress only, and at the toe-off event phase (TO) again there are three stresses axial compression, bending, and torsion (**Siddikali & Sreekanth, 2020**).

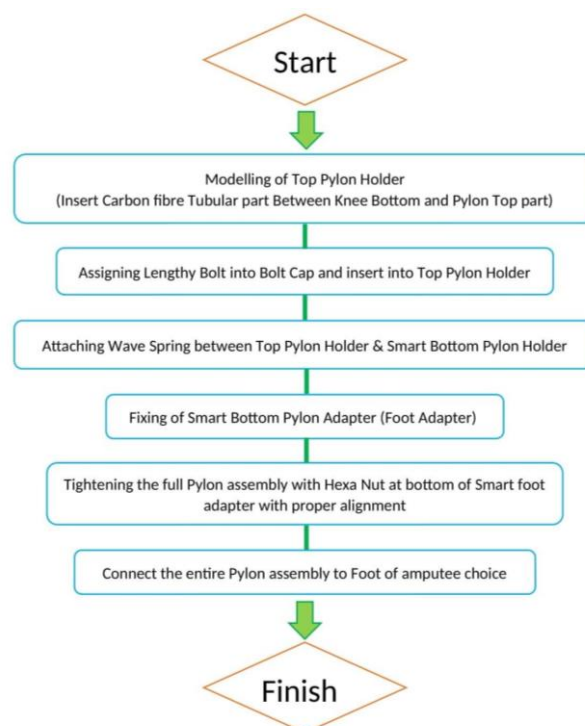


Figure. 2 Flowchart of Parametric Model of RSP

2.2. Regenerative effort assistive pylon with Smart foot adapter

The 'Regenerative effort assistive smart pylon (RSP) with Smart foot adapter (SFA) for high morale suspension for amble walk to reduce strain on to the amputee stump thereby preventing the wound or scar of the soft tissue of the stump. Whenever the amputee stump was not properly fit inside the socket it gets hurt because of lack of any suspension mechanism in the prosthetic leg while climbing the stairs (**Yu, Zhao, & Xu, 2011**), at present many commercially available prosthetic devices in the

market is lack retraction and regenerative effort to climb the stairs and which will only provide planar walk on the flat ground. This will diminish the full ability of the amputee which in turn reduces the self-confidence to move further and to carry out the daily activities, so this issue is precisely overwhelmed with the wave spring-suspended pylon for the conservation of the energy while placing the leg on the ground (**Meadows & Bowers, 2019**), and also the leg is removed from the ground with less effort by retraction force of wave spring thereby reducing the expenditure of metabolic energy of the user.

Integrated components such as adapters are used on either end of the pylon portion to attach the residual limb to the foot and a carbon fiber tubular piece is inserted in between the top pylon part and the bottom of the knee part for A/K amputees; in the case of adults during their lifespan, this usually may not change, but it may change rapidly for children and youth due to biological human development, which in turn changes the length and orientation of the prosthesis. This change in the prosthesis system as shown in Fig 3., taking into account the increased amputee loading regime, can produce higher torsion and bending moments on integral structural parts, which can lead to early failure if it is not properly balanced or replaced.

Heavier and larger amputee’s bionic system elements are known to have a shortened working life. As per the World Health Organization 2018 survey (**Roux & Laubscher, 2019**), 13 percent of the adult population was overweight and 39 percent were heavy (**Contacts, Abilitylab, Jayaraman, & Abilitylab, 2019**). Currently, the minimum duty life expected for the structural lower limb portion is approximately 3 million load cycles as recommended by ISO 10328:2016 (ISO-International Organisation for Standardization).

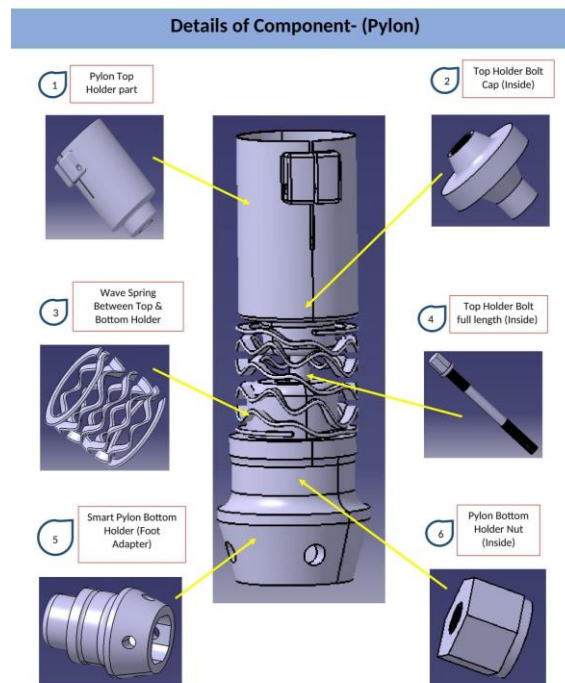


Figure. 3 Components of Regenerative effort assistive smart pylon

However, SFA as shown in Fig. 4, will promote a lot of physiological gait by enhanced gait stability, shortened step distance, and increased rollover. The extra transverse degree of freedom assists the

mentioned in Fig. 5. For simplification, when the Equations of equilibrium is applied by considering different individual masses of amputees for supposing (60 kg, 70 kg, 80 kg, 90 kg, and 100 kgs respectively), then based on the data ‘Winter data book’ (**Winter, n.d.**) for joint angles of the ankle concerning walking stride in percentage from 0 to 100 with 2 incremental for slow cadence, natural cadence and fast cadence of the amputees. Likewise, the GRF (considered in N/Kg) and Ankle force joint moment (considered in N.M/Kg), then by arranging the related values of all three cadences with related GRF in vertical and horizontal directions, ankle joint moment with the product of different masses of amputees to predict the stress minimum, $\sigma G (min)$ and stress maximum, $\sigma G (max)$ of stance event phase as mentioned in the below equation (3), where ‘theta’ is the angle of inclination of the pylon to the vertical axis. Fh & Fv are the GRF forces in horizontal and vertical directions. ‘ Mhv ’ gives the Ankle moment, the Center of Mass (COM) location can be obtained as: $vc = r \cos \theta$ and $hc = r \sin \theta$ in which vc and hc are the resolving forces as horizontal and vertical components and ‘ r ’ (0.06 meter) is the distance between below-knee connection to pylon moment at mid-stage phase. While considering the forces and moment for the pylon, the ankle area of the pylon is taken as ‘ A ’ and moment of inertia as ‘ I ’, where $d0$; outer diameter (as 0.033 meter) and di ; inner diameter (as 0.031 m) of pylon hollow cylindrical part. Then substituting in the below equation, σG :

$$\sigma G = \pm \frac{Fv \cos \theta - Fh \sin \theta}{A} \pm \frac{[(Fv \sin \theta - Fh \cos \theta) * r - Mhv] (\frac{d0}{2})}{I} \tag{1}$$

a) At Swing Event Phase (when the leg is off the ground):

$$\sigma G (min) = 0 \tag{2}$$

b) At Stance Event Phase (mid- stance phase):

$$\sigma G (max) = \frac{Fv \cos \theta - Fh \sin \theta}{\frac{\pi(d0^2 - di^2)}{4}} \pm \frac{[(Fv \sin \theta - Fh \cos \theta) * r - Mhv] (\frac{d0}{2})}{\frac{\pi(d0^4 - di^4)}{64}} \tag{3}$$

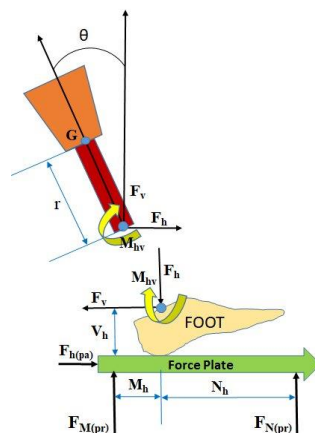


Figure. 5 Forces and moment with GRF on below-knee prosthetic

The above equations are obtained only for the stance phase σG (max) from heel-strike to toe-off (Houdijk et al., 2018) which completes 60 percent of the gait cycle and then substituted with proper values as mentioned above and its related graphs are obtained, and the remaining 40 percent was the swing phase of the leg which will be always considered as negligible forces

2.4.2. Direct, Bending, and Torsional stress equations

Sequentially for types of load with associated equations as detailed in Table 1. and mentioned in the article (Ávilaambriz et al., 2015), the choice of suitable joint definitions and parameter values, such as length and width of pylon unit, would result in satisfactory deflection or resistance to deflection on each axis.

Table.1. Stress type with corresponding equation and its directions

Load Type	Factors Involved	Corresponding equation
Axial (Direct)	F_v	$\sigma_d = \frac{P}{A}$
Bending	F_h	$\sigma_b = \frac{(M * y)}{I}$
Torsion	$M_h v$	$\sigma_t = \frac{(T * r_1)}{J}$

These are evaluated by considering the product of vertical GRF with resultant masses of amputees which were stated earlier is measured as load in the case of “Direct (axial stress- σ_d)” concerning the cross-sectional area. Similarly for “Bending stress” (σ_b), the product of the horizontal GRF with resultant masses of amputees at different cadence and the vertical distance from pylon mid-center to pylon top (r) with ‘ y ’ as the distance from the neutral axis of the pylon center to that of the outer diameter of the pylon for Moment of Inertia (I). Meanwhile, the “Torsional stress” (σ_t) is also calculated as the product of torque (T) of ankle force joint moment and radius (r_1) of the cylindrical pylon concerning the polar moment of inertia (J).

Aluminum alloys are among the conventional manufacturing materials that are considered and have been widely used. Numerous studies on fatigue-related material fractures have been reported and demonstrating the supremacy of aluminum-based composites over its matrix alloy in specific terms of fatigue strength, as well as improved yield and ultimate tensile strength. Especially, the fatigue behavior of artificially aged, powder metallurgy 6061 aluminum alloy, which is considered in the current study for the pylon material. The Physical properties and specific mechanical properties of the aluminum alloy are stated in Table 2.

Table.2. Mechanical properties of Aluminium (6061 T6)

Material	Yield Strength (S_y) (MPa)	Ultimate tensile Strength (S_{ui}) (MPa)	Endurance Limit (S_e) (MPa)
Al 6061	276	310	124

Based on all the chemical composition, physical, and mechanical properties; Al 6061 T6, is considered for the present study as it gives the best strength, stiffness with less weight. It is one of the materials which is easily available in the market and easily machinable (Lambrecht & Kazerooni, 2008) and it won't compromise with cost to weight ratio and perfectly suitable for the present work.

2.4.3. Stress-based Fatigue failure approach

To analyze the life-prediction and failure criteria of the present pylon device prone to high-cycle fatigue, where stress is mostly elastic, the stress-based fatigue approach is usually used. This approach emphasizes the nominal stress rather than the local stress. It measures the material stress-life curvature and uses fatigue notch factors to account for stress concentrations, practical modification factors for surface finishing effects, and empirical equations namely the modified Goodman (E. Osakue, Anetor, & Odetunde, 2015), Gerber, and ASME equations to compensate for mean stress effects. Stress Mean Vs Stress Amplitude curves are obtained for all associated failure parameters as mentioned (Guérinot, Magleby, Howell, & Todd, 2005). This study reveals that stochastic engineering models can be converted into probabilistic models that can forecast the risk of failure in a design scenario. The Modified Goodman, Gerber, and ASME-elliptic test for fatigue failure will be stressed from the design testing. The force pattern and the limits above and below a certain baseline can be described in a span of force (σ_{max} and σ_{min}). If the greatest and smallest force is σ_{max} and σ_{min} , then a steady function (Phanphet, Dechjarern, & Jomjanyong, 2017) (Stress mean- σ_m) and an alternating function (Stress amplitude - σ_a) can be formed. These correlation coefficients were established to create a line that defines an infinite-life modeling area. These relations produce curves, which link the endurance limit (S_e) upon its alternating stress axis to produce the yield strength (S_y), ultimate tensile strength (S_{ut}), or actual fracture stress on the mean stress axis.

Table.3. Modes of failure criteria and its fatigue factor of safety

Failure Criteria	Fatigue Factor of Safety (n_f)
Modified Goodman	$n_f = \frac{1}{\frac{\sigma_a}{S_e} + \frac{\sigma_m}{S_{ut}}}$
Gerber	$n_f = \frac{1}{2} \cdot \left[\frac{S_{ut}}{\sigma_m} \right]^2 \cdot \frac{\sigma_a}{S_e} \left[-1 + \sqrt{1 + \left[\frac{2\sigma_m \cdot S_e}{S_{ut} \cdot \sigma_a} \right]^2} \right], \sigma_m > 0$
ASME	$n_f = \sqrt{\frac{1}{\left[\frac{\sigma_a}{S_e} \right]^2 + \left[\frac{\sigma_m}{S_y} \right]^2}}$

($t = 1\text{mm}$) and the designed spring outer diameter ($OD = 33\text{mm}$) and internal diameter ($ID = 27\text{mm}$) and the mean diameter of the spring are ($D_m = 30\text{mm}$).

The wave spring is mounted unchanged by piloting on the lengthy bolt with a cap in between Top pylon part and the Smart pylon bottom foot adapter. The distance amongst the surfaces of loading defines the axial (vertical) working cavity or the wave spring's working height and the material of the spring's cross-section also has equal importance to the deflection of the overall design. The equations for the Operating stress (S_{op}), and spring rate (R_s) of wave spring areas are mentioned in Table 4. which will show why the Phosphor Bronze wave spring was chosen for the present work.

Consideration	Equation
Operating stress	$S_{op} = \left[\frac{(3\pi F * D_m)}{4w * t^2 * N^2} \right]$
Deflection	$f = \left[\frac{(F * K_m * n * D_m^3)}{(E * w * t^3 * N^4)} \right] * \left[\frac{ID}{OD} \right]$
Spring Rate	$R_s = \left[\frac{E * w * t^3 * N^4}{K_m * n * D_m^3} \right] * \left[\frac{ID}{OD} \right]$

Table.4. Stress consideration and its equations.

Results and Discussions

In the present work stress distribution along with the RSP pylon for different masses of amputees during the gait walk cycle has been calculated. For finding out the maximum stress ($\sigma_{G(max)}$) concentration after the heel strike on the force plate and the maximum value of stress are obtained during the mid-stance phase where the prosthetic leg with fitted RSP pylon will be in an upright position and the extreme body mass of the amputee will fall on to the pylon. At this phase based on the stress maximum equation, the related joint angle (theta) of the ankle is counted, the product of vertical ground reaction force vector with amputee mass and as well as horizontal ground reaction force vector with amputee mass was calculated to find out the GRF-theta values respectively. Also, the product of joint moment to amputee mass is considered, the distance between below-knee connection to pylon moment at mid-stage phase, (r) as stated above is taken and all these values as mentioned are substituted in the $\sigma_{G(max)}$ equation for stance phase and it is at peak value during the mid-stance and it was represented for the stress maximum versus gait cycle with the help of plotting the graphs Fig. 7, for all the different masses of amputees varying from 60 kg to 100 kg, with 10 kg increments during slow cadence, the natural and fast cadence of the gait cycle. The stress maximum (Phanphet et al., 2017) obtained during the slow cadence (walk) as 26.50, 30.91, 35.33, 39.75, and 44.16 MPa, similarly for a natural cadence (37.05, 43.23, 49.40, 55.58, and 61.75 MPa, likewise for a fast cadence (47.31, 55.20, 63.08, 70.97, and 78.85 MPa). Here we can notice that when the mass of the amputee increases the Stress maximum also increasing in each cadence and this will complete 60 percent of the gait cycle and the remaining was the swing phase and very negligible stress concentration will be there on the pylon during this phase. Fig. 7, pertaining to the stress distribution with the gait cycle for the stance phase with respect to the percentage of stride for different masses of amputees. Maximum stress is at the heel strike then dropping gradually at mid-stance then it is not

Design verification of optimized regenerative pylon with smart foot adapter for socio-economic backward classes with lower limb amputation

expected during the swing phase where the leg will be off the ground, again it will increase when the heel strikes. The value of stress is alternating due to the change in GRF.

For finding the 'Direct stress' of (0 to 100 percentage stride) during slow cadence based on the corresponding equation after substitution of the above-mentioned terms, the related maximum direct stress values for different masses of amputees are 5.97, 6.97, 7.96, 8.96, and 9.96 MPa, similarly for natural cadence is 6.46, 7.53, 8.61, 9.69 and 10.76 MPa. Likewise, for a fast cadence, the values are 7.56, 8.82, 10.08, 11.34, and 12.60 MPa.

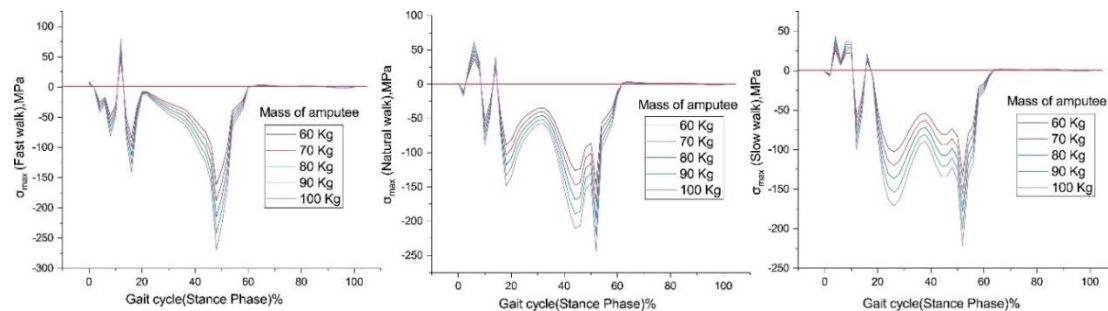


Figure. 7 Stress maximum in RSP Pylon during Gait walk a) Fast b) Natural c) Slow walk for different masses of amputee

Same as the Direct stress, the 'Bending stress' values are based on the equations analytical values for a slow cadence as 7.33, 8.55, 9.78, 11.00, and 12.22 MPa, for a natural cadence as 10.10, 11.78, 13.47, 15.15 and 16.84 MPa and related values for the fast cadence are 11.85, 13.83, 15.81, 17.78 and 19.76 MPa.

The corresponding 'Torsional stress' values for slow cadence are 59.02, 68.85, 78.69, 88.53, and 98.36 MPa. Similarly for natural cadence 62.59, 73.02, 83.46, 93.89, and 104.32 MPa. Likewise, for fast cadence, the values are 66.94, 78.09, 89.25, 100.41, and 111.56 MPa.

Deformation in the pylon by axial compression, bending, and torsion due to an amputee body mass of approximately 60-100 kgs respectively at varying cadence, by taking into account the forces in the longitudinal, horizontal direction and for the particular moment and rotation, may result in a beam/pylon that would collapse due to high tension at the fixed support (**Series & Science, 2018**) of the beam. The theoretical approximation for the RSP has thus been performed to pre-forecast the existence of the novel pylon. Approximation of the propulsion phase effectively from 0 to 60 percent of the standing position for different masses of amputees during the gait cycle is measured and cross-checked with axial, bending, and torsional equations to produce the associated graphs as shown in Fig. 8, Fig. 9, and Fig. 10 of fast, normal, and slow walking and obtained as stresses in MPa. These stresses are considered very carefully because this may cause failure in the pylon when neglected and it may compress, twist, and bend the pylon during true gait walk, but for this RSP pylon, it is under the limiting condition.

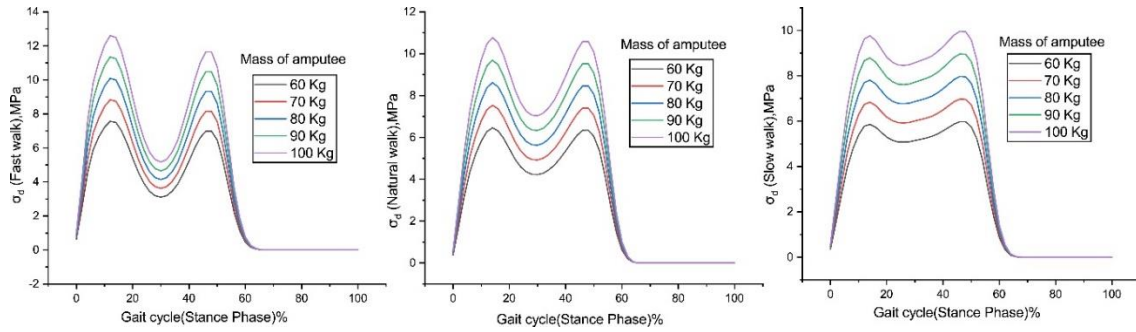


Figure. 8 Direct Stress during Gait walk generated in RSP Pylon during a) Fast b) Natural c) Slow walk

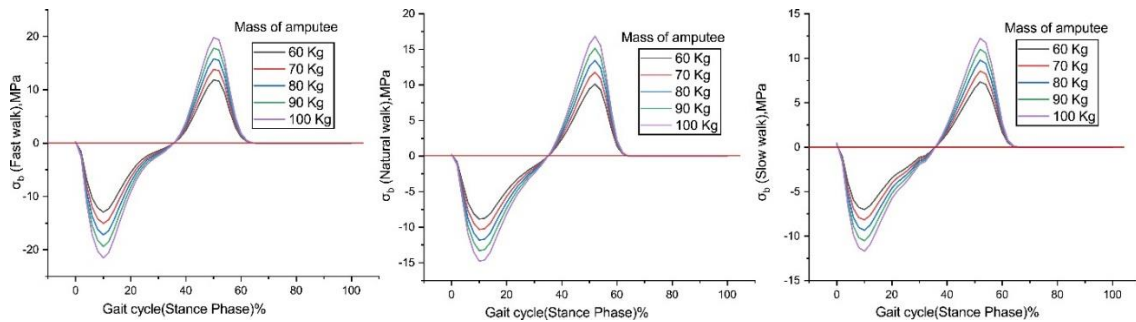


Figure. 9 RSP Pylon reaction due to Bending Stress during a) Fast walk b) Natural walk c) Slow walk

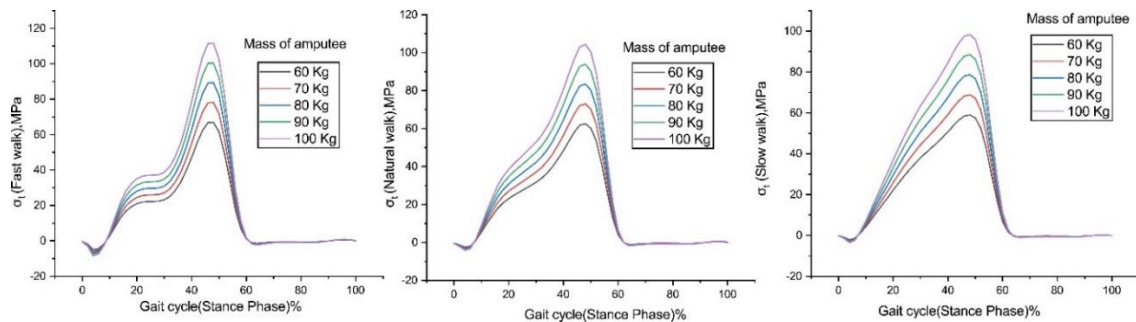


Figure. 10 Torsional Stress in RSP Pylon during Gait walk a) Fast b) Natural c) Slow

In this study to find out the fatigue factor of safety, the product of vertical GRF and related masses of amputees which were stated earlier is taken into consideration and is divided into five phases (Schuy et al., 2020) for slow, natural, and fast cadence for amputee masses. The resultant values of each phase for different masses of amputees concerning cadence are characterized to find the force patterns in ranges for the largest force (σ_{max}) and smallest force (σ_{min}), then its related steady component (σ_m) and alternating components (σ_a) are generated for cross-sectional area (A) of pylon by considering the highest (σ_{max}) and lowest (σ_{min}) of all 5 phases for each mass of amputee substituted in the intersecting fatigue criteria equations as tabulated in Table 3. and the final ‘fatigue factor of safety; n_f ’ for failure criteria’s of Modified Goodman as ($n_f = 2.07$), Gerber ($n_f = 2.55$) and ASME ($n_f = 2.65$) are obtained which has suggested the failure risk in the newly designed RSP pylon part is very minute and it is noted that the Modified Goodman, Gerber and the ASME-

Design verification of optimized regenerative pylon with smart foot adapter for socio-economic backward classes with lower limb amputation

elliptic fatigue failure criteria are very close to each other and are used interchangeably and states that the designed model is very less prone to failure risk in real-time working condition.

To find the maximum ‘operating stress’, deflection of the spring will be counted at the mid-stance phase of the prosthetic leg, where the amputee body weight will descent on the pylon part of the prosthetic leg when the intact leg will be in the swing phase (off the ground). Because of the pylon with wave spring regenerative effort assistive mechanism, the spring compresses to its maximum and stores energy based on the load of the amputee and then retracts to its initial position and regenerates the stored energy when at the time of Toe-off event and it will stay unchanged in the swing phase. For the ‘operating stress’ (S_{op}), the product of vertical GRF will be considered along with different masses of amputees of ranges from 60 kg to 100 kg with 10 kg increments in slow, natural, and fast cadence and substituted in the mentioned equation and related graphs are plotted Fig. 11 and Fig. 12. It is observed that the maximum operating stress during ‘slow cadence’ with different masses (60-100 kgs respectively) of amputee are 884.00, 1031.34, 1178.67, 1326.01, and 1473.34 MPa. Similarly for ‘natural cadence’ as 955.54, 1114.79, 1274.05, 1433.31, and 1592.56 MPa. In the same way for ‘fast cadence,’ the values are 1118.91, 1305.40, 1491.89, 1678.37, and 1864.86 MPa.

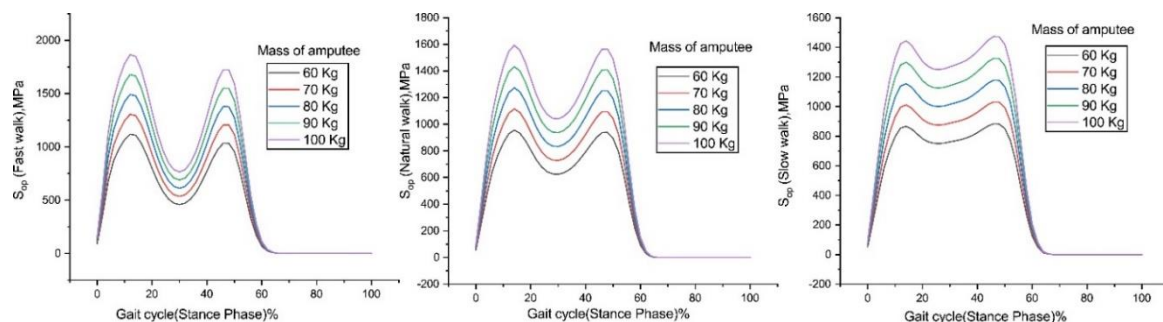


Figure. 11 Operating stress (S_{op}) in the wave spring during Gait walk for different masses of amputee a) Slow b) Normal c) Fast

Similarly, the maximum ‘spring deflection’ was calculated for the above-mentioned condition and it was found that during ‘slow cadence’ of an amputee, the respected values are 0.0039, 0.00455, 0.00520, 0.00585 and 0.0065 mm.

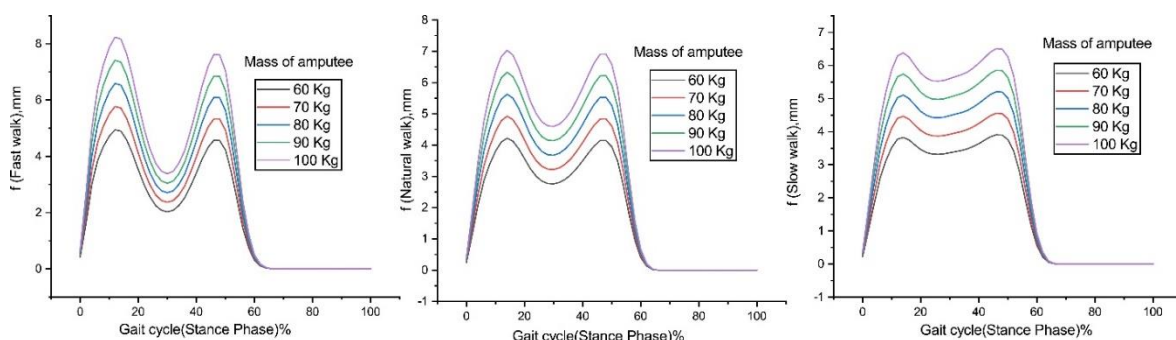


Figure. 12 Deflection in Wave spring (f) during gait walk for different masses of amputee a) Slow walk
b) Normal Walk c) Fast Walk

Likewise for 'natural cadence' 0.0422, 0.0492, 0.0562, 0.0633, and 0.0703 m. For 'fast cadence' the maximum deflection (Abdullah, Wasmi, & Saad, 2017) values are 0.0494, 0.0576, 0.0658, 0.0741, and 0.0823 m. It is noted that whenever the load increases the deflection in the wave spring also changes accordingly. The overall spring constant (R_s) was estimated as 102960 N/m for wave spring's young's modulus of (14938887 psi), where the material is 'Phosphor Bronze'. The plotted graphs show that the operating stress will be more when the mass of the amputee increases and as well as the deflection of the wave spring also increases gradually. The fatigue safety factors for Pylon are under the prescribed limit, this is due to the cross-sectional area of the pylon part and material mechanical properties for the RSP pylon.

The impact response during heel strike to mid-stance reveals that the RSP pylon coupled with wave spring and SFA can take the high impact stresses and the force transfers through the pylon to the ground, during real gait walk and due to the wave spring it will also absorb the energy during heel strike and releases the energy during toe-off. The final results indicate that the RSP pylon is less stiff and wave spring is lenient for the forces and dissipates more impact energy and it might be considered for walking gait similarity, therefore we can notice minimized force transmission when the advanced RSP pylon is considered instead of a regular tubular pylon.

4. Conclusion

In the present work, the novel regenerative effort assistive pylon with smart foot adapter has been designed with all the specific dimensions and can perfectly fit any of the prosthetic knee joints which are commercially available in the market with proper adapters and mountings. Various amputee patients with different weights varying from 60-100 kgs have been considered and all the designed components are validated for their strength and stiffness on different criteria as mentioned in results and discussions. The following are the conclusions based on the current study.

1. The 'Novel regenerative effort assistive smart pylon' is less stiff but can dissipate more energy where the regular tubular pylon can't do this.
2. The body force and the GRF forces are absorbed with the help of wave spring arrangement and regenerated when required and the device is lighter and stronger.
3. RSP with SFA is an innovative concept that will comfort the A/K amputees when used with knee parts or for B/K amputees without knee parts and safeguard the amputee during gait without having fear of falling.
4. The presence of SFA at the bottom of RSP favors the longevity of walk and it was proved that it is more resistant to fatigue and fracture and makes it a good alternative pylon to reduce the energy consumption of amputees during walking gait.
5. RSP is much useful for young/ elderly people during stair climbing and descending and can be made economical when manufactured and can be easily fitted to the amputees.

References

- [1]. Abdullah, M. Q., Wasmi, H. R., & Saad, H. (2017). The Modeling and Effect of FEM on Prosthetic limb. *International Journal of Cell Science and Biotechnology International Journal of Current Engineering and*

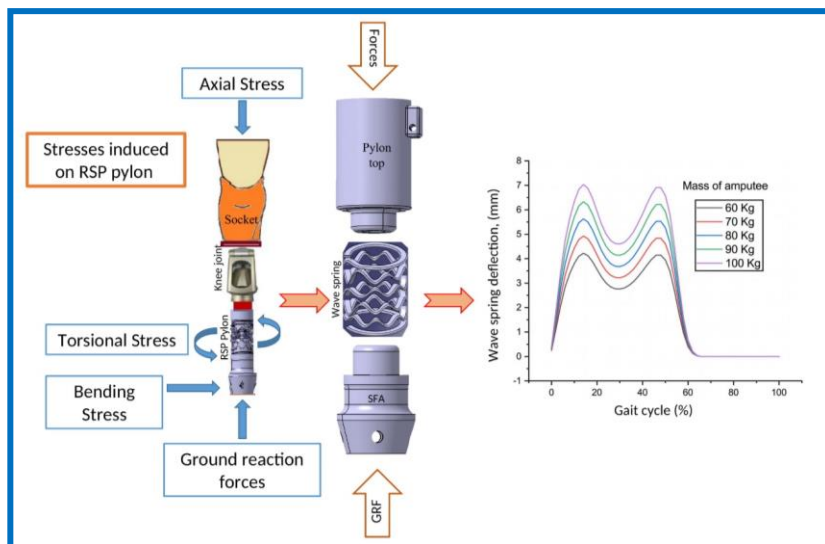
Design verification of optimized regenerative pylon with smart foot adapter for socio-economic backward classes with lower limb amputation

- Technology*, 77(33), 2320–7574. Retrieved from <https://www.researchgate.net/publication/316940800%0Ahttp://inpressco.com/category/ijcsb/>
- [2]. Ávilaambriz, J. L., Almaraz, G. M. D., Gómez, E. C., & Juárez, J. C. V. (2015). Fatigue Endurance Under Rotating Bending and Torsion Testing , of AISI 6063-T5 Aluminum Alloy. *International Journal of Advanced Materials Research*, 1(4), 120–125.
- [3]. Buckley, J. G., Jones, S. F., & Birch, K. M. (2002). Oxygen consumption during ambulation: Comparison of using a prosthesis fitted with and without a tele-torsion device. *Archives of Physical Medicine and Rehabilitation*, 83(4), 576–581. <https://doi.org/10.1053/apmr.2002.30624>
- [4]. Collins, S. H. (2008). Dynamic walking principles applied to human gait. *Mechanical Engineering, PhD*, 116.
- [5]. Contacts, S., Abilitylab, S. R., Jayaraman, A., & Abilitylab, S. R. (2019). Impact of Powered Knee-Ankle Prosthesis Leg on Everyday Community Mobility and Social Interaction.
- [6]. de Jong, L. A. F., Kerkum, Y. L., van Oorschot, W., & Keijsers, N. L. W. (2020). A single Inertial Measurement Unit on the shank to assess the Shank-to-Vertical Angle. *Journal of Biomechanics*, 108, 109895. <https://doi.org/10.1016/j.jbiomech.2020.109895>
- [7]. E. Osakue, E., Anetor, L., & Odetunde, C. (2015). Fatigue Shaft Design Verification for Bending and Torsion. *International Journal of Engineering Innovation & Research*, ISSN: 227-5668, 4(1), 197–206.
- [8]. Guérinot, A. E., Magleby, S. P., Howell, L. L., & Todd, R. H. (2005). Compliant joint design principles for high compressive load situations. *Journal of Mechanical Design, Transactions of the ASME*, 127(4), 774–781. <https://doi.org/10.1115/1.1862677>
- [9]. Houdijk, H., Wezenberg, D., Hak, L., & Cutti, A. G. (2018). Energy storing and return prosthetic feet improve step length symmetry while preserving margins of stability in persons with transtibial amputation. *Journal of NeuroEngineering and Rehabilitation*, 15(Suppl 1). <https://doi.org/10.1186/s12984-018-0404-9>
- [10]. Jacobs, N. A. (1998). Prosthetics and orthotics international: Editorial. *Prosthetics and Orthotics International*, 22(3), 177. <https://doi.org/10.3109/03093649809164481>
- [11]. Jweeg, P. M. J., & Mohammed, M. N. (n.d.). Design And Manufacturing Of A New Prosthetic Low Cost Pylon For Amputee Abstract : 2 . Modeling Human Walking And Mathematical Analysis Of The Pylon :
- [12]. Kadhim Oleiwi, J., & Jumaah Ahmed, S. (2016). Tensile and Buckling of Prosthetic Pylon Made from Hybrid Composite Materials. *&Tech.Journal*, 34(14).
- [13]. Kim, S., Ro, K., & Bae, J. (2017). Estimation of individual muscular forces of the lower limb during walking using a wearable sensor system. *Journal of Sensors*, 2017. <https://doi.org/10.1155/2017/6747921>
- [14]. Koehler-mcnicholas, S. R., Lipschutz, R. D., & Gard, S. A. (2016). Variations in Prosthetic Knee Alignment During Level Walking, 53(6), 1089–1106. <https://doi.org/10.3389/fbioe.2015.00209>
- [15]. Lambrecht, B. G. A., & Kazerooni, H. (2008). Design of a hybrid passive-active prosthesis for above-knee amputees, 3353425, 115. <https://doi.org/10.1007/s13398-014-0173-7.2>
- [16]. Lin, H., Hwang, J. R., & Fung, C. P. (2016). Fatigue properties of 6061-T6 aluminum alloy butt joints processed by vacuum brazing and tungsten inert gas welding. *Advances in Mechanical Engineering*, 8(4), 1–13. <https://doi.org/10.1177/1687814016643454>
- [17]. Marno, M., & Ismail, A. badri. (2012). Torsional Deformation and Fatigue Behaviour of 6061 Aluminium Alloy. *IJUM Engineering Journal*, 12(6), 21–32. <https://doi.org/10.31436/iiumej.v12i6.145>
- [18]. Meadows, B., & Bowers, R. (2019). 18 - *Biomechanics of the Hip, Knee, and Ankle. Atlas of Orthoses and Assistive Devices* (Fifth Edit). Elsevier Inc. <https://doi.org/10.1016/B978-0-323-48323-0.00018-4>
- [19]. Pavani, P. N. L., Prafulla, B. K., Rao, R. P., & Srikirana, S. (2014). Design, Modeling and Structural Analysis of Wave Springs. *Procedia Materials Science*, 6(Icmpc), 988–995. <https://doi.org/10.1016/j.mspro.2014.07.169>
- [20]. Pejhan, S., Farahmand, F., & Parnianpour, M. (2008). Design Optimization of an Above-Knee Prosthesis Based on the Kinematics of Gait, (February). <https://doi.org/10.1109/IEMBS.2008.4650154>
- [21]. Phanphet, S., Dechjarern, S., & Jomjanyong, S. (2017). Above-knee prosthesis design based on fatigue life using finite element method and design of experiment, 0, 1–6. <https://doi.org/10.1016/j.medengphy.2017.01.001>
- [22]. Roux, P. A., & Laubscher, R. F. (2019). Approach to Enhance the Fatigue Life of a, (November), 47–54.
- [23]. Schuy, J., Stech, N., Harris, G., Beckerle, P., Zahedi, S., & Rinderknecht, S. (2020). A Prosthetic Shank With Adaptable Torsion Stiffness and Foot Alignment. *Frontiers in Neurorobotics*, 14(May), 1–13. <https://doi.org/10.3389/fnbot.2020.00023>
- [24]. Series, I. O. P. C., & Science, M. (2018). Design And Manufacturing Knee Joint for Smart Transfemoral

Prosthetic Design And Manufacturing Transfemoral Prosthetic Knee Joint for Smart. <https://doi.org/10.1088/1757-899X/454/1/012078>

- [25]. Siddikali, P., & Sreekanth, P. S. R. (2020). Materials Today : Proceedings Modeling of pneumatic controlled bio mimetic articulated passive prosthetic spring loaded knee mechanism for transfemoral amputees. *Materials Today: Proceedings*, (xxxx). <https://doi.org/10.1016/j.matpr.2019.12.377>
- [26]. Soni, M., Maji, S., & Anand, S. (2010). 548. Modelling an above knee prosthesis-a kinematics approach. *Journal of Vibroengineering*, 12(2), 215–224.
- [27]. Tekwani, H. C., & Joshi, D. D. (2018). Effect of Load variation and thickness on deflection and operating stress of wave spring. *International Journal of Trend in Scientific Research and Development*, Volume-2(Issue-4), 684–689. <https://doi.org/10.31142/ijtsrd13057>
- [28]. Winter, D. A. (n.d.). *The Biomechanics and Motor Control of Human Gait*.
- [29]. Yu, H. L., Zhao, S. N., & Xu, Z. H. (2011). Study on the usability evaluation of prosthetic leg products based on ergonomics. *Journal of the Brazilian Society of Mechanical Sciences and Engineering*, 33(3), 366–372.

Graphical Abstract:



Vellore Institute of Technology-Andhra Pradesh

Amaravati, Andhra Pradesh - 522 237, India. Web : www.vitap.ac.in

Letter to the Editor

Sub: Submission of a manuscript

Dear Dr. Esra Sipahi,

Enclosed please find a manuscript entitled “Design verification of optimized regenerative pylon with smart foot adapter for socio-economic backward classes with lower limb amputation” by P Siddikali & P S Rama Sreekanth, to be considered for publication in ‘Turkish Online Journal of Qualitative Inquiry’.

Design verification of optimized regenerative pylon with smart foot adapter for socio-economic backward classes with lower limb amputation

The work elaborates the need for Regenerative effort assistive Smart Pylon (RSP) with Smart foot adapter (SFA) and a wave spring suspension mechanism for stance position to discover the distribution of stresses, its related deformation, and to withstand under static and dynamic impact loading conditions during the gait cycle by considering different masses of amputees varying from 60-100 kgs. This innovative design stabilizes the amputee to ground reaction forces (GRF) without falling. Stress maximum, axial, bending, and torsional stresses were assessed and the related fatigue failure criteria were evaluated for the pylon and the operating stress, deflection response, and spring rate of the wave springs have been identified. It was concluded that the novel RSP with SFA is more favorable for lower limb amputees to facilitate them to carry out their daily activities without compromising. The authors believe that the reported work is novel and unique and would be of interest in the field of relevance.

I would like to confirm that no conflict of interest exists in the submission of this manuscript, this is approved by all authors for publication. I would like to declare on behalf of my co-authors that the work described was original research that has not been published previously, and not under consideration for publication elsewhere, in whole or in part, and will not be submitted elsewhere before a decision is made. All the authors listed have approved the manuscript that is enclosed.

May I request you to kindly do the needful, Thank you and best regards.

Yours sincerely,

P. S. Rama Sreekanth, Ph.D